Entropic Character of the Atomic Level Stress in Polymeric Melts

R. C. Picu

Department of Mechanical Engineering, Aeronautical Engineering and Mechanics, Rensselaer Polytechnic Institute, Troy, New York 12180

Received December 22, 2000; Revised Manuscript Received April 9, 2001

ABSTRACT: The entropic character of the atomic level stress in polymeric melts and the stress optical coefficient are studied in model systems by the use of equilibrium and nonequilibrium molecular dynamics. The atomic level stress is defined in intrinsic coordinates, a mobile frame tied to the generic bond. The global stress σ is obtained in the global coordinate system by summing up the contributions due to the intrinsic stress corresponding to each atom in the population. The atom-based global stress is proportional to an average measure of bond orientation (P_2), with the proportionality constant σ/P_2 being related to the macroscopic stress optical coefficient (SOC). The proportionality constant may be expressed in terms of intrinsic quantities which, in turn, are computable from equilibrium simulations. The model reproduces most experimentally observed properties of the SOC. The ratio σ/P_2 is chain length and deformation rate independent in the melt and becomes rate dependent in the glassy state. The dependence of the global stress on temperature at imposed average bond orientation is therefore determined by the variation of the intrinsic stresses with temperature. The stress is purely entropic in the melt for all chain lengths. However, neither one of its components, that due to bonded and that due to nonbonded interactions, is purely entropic. The global stress σ acquires an energetic component at high temperatures and at large deformations, when chains are significantly stretched. The entropic character of the atomic level stress is shown to be due to packing effects, similar to the situation encountered in simple fluids. These conclusions remain unchanged upon variation of the model parameters such as the stiffness of the nonbonded and bonded interatomic potential, the cutoff radius of the nonbonded potential, and the bond length.

1. Introduction

Stress production in polymeric systems is generally understood, at present, to be based on a model in which chains are regarded as entropic springs in tension.[1−3] The configurational entropy variation associated with stretching a chain leads to a retractive force or a stress on the material scale. Stress is due to bonded interactions only, while nonbonded interactions lead to a hydrostatic component.

This article is part of an ongoing effort to understand stress production and relaxation starting from the atomic interactions rather than by the use of the entropic spring concept.[4−10] Similar atomic-scale studies have been performed by Fixman[11] and Kroger et al.[12] In this "intrinsic framework", stress is computed on the atomic level by explicitly considering both bonded and nonbonded interactions. The contribution to stress of nonbonded interactions was shown to be more significant than that of bonded interactions. The intrinsic stress is the stress associated with an atom and projected in a coordinate system tied to the respective bond of the chain. The intrinsic coordinate system is therefore mobile, and the macroscopic stress is given by the sum of "stresslets" (intrinsic stress tensor) rotated in the global coordinate system.[10] Interestingly, it was observed that the intrinsic stress tensor is insensitive to the deformation of the melt and is therefore a system parameter for given thermodynamic conditions. Furthermore, the stress−optical coefficient (SOC), representing here the ratio of a measure of bond orientation $P_2 = {}^1/_2\langle 3\cos^2\theta_b - 1\rangle$ (θ_b is the angle defining bond orientation) to the global stress, may be expressed in terms of intrinsic stresses.[7,13,14] It must be noted that the definition used here for the SOC is slightly different than the macroscopic definition where the SOC is the ratio of birefringence to the global stress. These remarkable properties support the further development of the model.

In the new formulation, stress is due to excluded-volume effects on the atomic scale (steric shielding).[10] As is obvious from the above discussion, this interpretation is at odds with the entropic spring model in which the stress is defined on the molecular level. In the classical formalism, the stress is, by definition, entropic. This is in agreement with experimental observations. It then becomes necessary to determine whether the intrinsic framework captures this property or, in particular, whether the intrinsic stress is entropic. If this is the case, the physical origin of the entropic character of the intrinsic stress must be revealed. This investigation is the object of the present study.

Before proceeding to the analysis, it is necessary at this point to review the primary established features of the SOC since, as noted above, the global stress may be expressed in terms of SOC and P_2.[14]

At temperatures above T_g + 20 °C, the SOC is measured to be essentially deformation rate independent, and at low stresses, it is also independent of the magnitude of the applied stress.[12,15] It has been reported, however, that measurements of birefringence are problematic at very low strain rates due to intense relaxation, the threshold rate at which measurements could be performed being dependent on the molecular weight and on the presence of a solvent.[16] Furthermore, large stresses cause significant chain alignment, and the ratio of birefringence to stress decreases with increasing applied stress.

At large temperatures, in the melt state, the measured SOC is independent of temperature even in the nonlinear part of the SOC-stress dependence.[15] At lower

10.1021/ma002186s CCC: $20.00
Published on Web 06/02/2001

temperatures and in some material systems, the SOC becomes temperature sensitive.[16,17] At the glass transition, the SOC exhibits a significant variation and becomes essentially constant with temperature below the transition.[17]

Stress has both an entropic and an energetic component. The entropic component dominates at high temperatures, while in the glassy state and at high deformation rates the stress is predominantly energetic. The intrinsic framework is able to capture most of these properties as discussed in the following section.

The outline of the paper is as follows: a description of the model and the algorithm employed are presented in section 2, and an overview of the intrinsic framework is presented in section 3, while in section 4, the entropic vs energetic nature of stress is discussed. The conclusions are summarized in section 5.

2. Model Description

The present investigation is based on computer simulation of model systems consisting of dense collections of molecules. The molecules are represented by a "pearl necklace" type model in which particles represent atoms linked into chains by stiff linear springs simulating covalent bonds. Short molecules of four atoms per chain as well as long chains (200-atom chains) are considered. The covalent bond between the pair of atoms of each molecule is represented by the potential

$$u_b(r) = \frac{1}{2}\kappa(r - b_0)^2 \tag{1}$$

and all nonbonded atoms interact with a truncated Lennard-Jones potential. Here r denotes the distance between any pair of atoms and b_0 is the bond length. The spring constant κ has a value corresponding to $\kappa b_0^2/k_BT = 267$, while $b_0 = 1$, unless specified otherwise. In the present simulations, the nonbonded interactions are represented by a purely repulsive Lennard-Jones potential with cutoff radius $R_c = 2^{1/6}$ (WCA potential). Additional simulations have been performed with a larger cutoff radius. The units of the problem are those imposed by the Lennard-Jones potential.

Periodic boundary conditions are used in the simulations as is customary in molecular dynamics. The basic cell referred to a Cartesian system is, in the equilibrium state, a cube of dimensions L. There are N atoms per unit cell, which leads to a reduced density $\rho = N/L^3$. The simulation begins with the atoms being arranged in an fcc pattern and with a random velocity field. A high-temperature equilibration is performed to obtain a proper melt structure. In simulations of short chain molecules (four-atom chains), the system was composed from $N = 632$ atoms, while long-chain systems (200-atom chains) contained $N = 4025$ atoms.

The algorithm used to integrate the equations of motion as well as the thermostat are those due to Berendsen et al.[18] The position of a particle at time $(t + \Delta t)$ is obtained from its position at time t and that at $(t - \Delta t)$ by

$$\mathbf{x}(t + \Delta t) = (1 + \xi)\mathbf{x}(t) - \xi\mathbf{x}(t - \Delta t) + \xi\frac{f}{m_0}\Delta t \tag{2}$$

where the force $\mathbf{f}$ acting on the atom in question is determined from the atomic positions at time t. The scaling factor ξ is given by the equation

$$\xi = \left[1 + \frac{\Delta t}{\Omega}\left(\frac{T_0}{T(t - \Delta t/2)} - 1\right)\right]^{1/2} \tag{3}$$

where T_0 is the target temperature and $T(t - \Delta t/2)$ is calculated on the basis of the velocities at time $(t - \Delta t/2)$ obtained from

$$\mathbf{v}(t - \Delta t/2) = \frac{\mathbf{x}(t) - \mathbf{x}(t - \Delta t)}{\Delta t} \tag{4}$$

The parameter Ω controls the speed of response of the algorithm to a temperature perturbation. For our simulations performed under high strain rate−high energy input conditions, this parameter is taken as $\Omega = 10\Delta t$. For this value it was verified that the temperature at the onset of relaxation is the target temperature and remains so through the remaining relaxation. The time step of integration Δt is kept constant for the whole loading−relaxation history and equal to 0.001. It was verified that further decrease in Δt did not affect the results.

Simulations are performed under both equilibrium and nonequilibrium conditions. In nonequilibrium runs, the deformation of the melt is induced by a volume-preserving elongational deformation of the unit cell. During such a deformation, with the stretch direction x_1, the cell size is modified according to

$$\begin{aligned} L_1 &= L(1 + \dot{\epsilon}t) \\ L_2 &= L/(1 + \dot{\epsilon}t)^{1/2} \\ L_3 &= L/(1 + \dot{\epsilon}t)^{1/2} \end{aligned} \tag{5}$$

where $\dot{\epsilon}$ is the deformation strain rate. All simulations reported here are performed with a strain rate $\dot{\epsilon} = 0.1$, and the total deformation of the cell in the stretch direction is 10%. The periodic boundary conditions remain unchanged during deformation.

To reduce the noise in measured quantities, the calculation has to be repeated N_c number of times using independent initial conditions, and the results are averaged over all runs. The results reported here are obtained by averaging over $N_c = 100$ simulations for the short chain system and over $N_c = 12$ simulations for the 200-atom chain system. A larger number of replicas ($N_c = 600$) had to be considered for the computations of the D constant (see below).

3. Overview of the Intrinsic Stress Framework

Atom-Based Stress and Distributions. The stress t_{ij} in the melt expressed in the global coordinate system tied to the simulation cell is computed using the virial stress formula[19]

$$vt_{ij} = -NkT\delta_{ij} + \frac{1}{2}\sum_{m=1}^{N}\langle\sum_{n=1}^{N_m} r_{mn}^{-1}u'_{mn}(r_{mn})r_{mni}r_{mnj}\rangle \tag{6}$$

where $v = L^3$ is the volume of the unit cell, r_{mn} is the length of the vector $\mathbf{r}_{mn}$ between interacting atoms m and n and has components r_{mni}, and $u' = du/dr$. The first sum is taken over all atoms in the system while the second is over all N_m atoms interacting with atom m at time t in a given simulation. The contribution to stress of both bonded and nonbonded interactions is consid-

ered, with u_{mn} representing the respective potential. The kinetic contribution $-NkT$ is assumed to affect the hydrostatic stress only since the thermal velocities are much higher than those due to deformation (in nonequilibrium). The angular bracket represents time averaging in an equilibrium simulation and averaging over all N_c simulations (trajectories) in nonequilibrium.

The nonkinetic contribution to global stress of a representative atom m, at time t and in a given simulation, is therefore

$$\sigma_{ij}^{m} = \frac{1}{2v}\sum_{n=1}^{N_m} r_{mn}^{-1} u'_{mn}(r_{mn}) r_{mni} r_{mnj} \tag{7}$$

The intrinsic stresses are defined for each atom, in an intrinsic coordinate system $\tilde{x}_r$ with axis $\tilde{x}_1$ tied to one of the covalent bonds of that atom.[9] The atomic level stress due to atom m in eq 7 may be expressed in the intrinsic coordinate system by a simple rotation of the stress tensor as

$$\tilde{\sigma}_{rs}^{m} = \sigma_{ij}^{m} a_{ri}^{m} a_{sj}^{m} \tag{8}$$

where $a_{ri}^{m} = \mathbf{a}_r^m \cdot \mathbf{e}_i$ are components of the rotation matrix relating the global and intrinsic coordinate systems for atom m. The intrinsic stress tensor $\tilde{\sigma}_{rs}$ is obtained by averaging $\tilde{\sigma}_{rs}^{m}$ over all N atoms in the system and over all N_c simulations.

The intrinsic stress is a cylindrical tensor in which the only nonzero components are $\tilde{\sigma}_{11}$ and $\tilde{\sigma}_{22} = \tilde{\sigma}_{33}$. Most remarkably, it was observed that, when computed from atoms which are not at the chain ends, its components are independent of chain length.[4] The dependence of the intrinsic stress on the position of the representative atom on the chain was studied by Gao and Weiner.[14] Furthermore, the intrinsic stress tensor computed from equilibrium simulations has the same value as that computed from nonequilibrium simulations, except for a small variation during loading.[7]

The relationship between intrinsic stresses and the atomic structure about a representative atom was studied in the intrinsic coordinate system $\tilde{x}_r$ by using an intrinsic distribution function $\tilde{g}(\tilde{r},\tilde{\theta})$.[8] This function is similar to the standard radial distribution function $g(r)$ defined in the global coordinate system x_i. As a point of difference, $\tilde{g}$ is not isotropic (constant in the $\tilde{\theta}$ direction) due to the steric shielding. This leads to a nonzero deviatoric intrinsic stress. The intrinsic distribution was shown to behave similarly with the intrinsic stresses; i.e., it is chain length independent (when computed from chain inner atoms) and is independent of melt deformation during the α relaxation regime. A review of earlier work on the concept of steric shielding and its importance is presented by Gao and Weiner.[10]

Stress Relaxation. Stress relaxation was studied in this system in nonequilibrium simulations.[7] The picture offered by the atom-based stress decay is similar to that commonly observed in experiments for stress at the macroscopic scale. At early times (or high frequencies), the β-mode is dominant, and the stress drops sharply following a power law relaxation. The subsequent modes (or at low frequencies) are of the α-type, are much slower, and may be described by a Prony series. The intrinsic stress has a small variation during the β mode. At later times, during the α relaxation, the intrinsic stress tensor becomes time-independent. Stress during the β mode has a pronounced energetic character, while during the α mode it is essentially entropic.

Each mode of stress relaxation may be associated with specific atomic-scale structural changes in the fluid.[13] During deformation, the close neighborhood of a representative atom (the "cage") becomes anisotropic. Consequently, the pair distribution function $g(r)$ becomes direction dependent, or the "cage" becomes elliptical. Furthermore, the bond orientation distribution is rendered anisotropic. The return to isotropy of these structural measures during relaxation is directly related to the various relaxation modes. The return to isotropy of the "cage" takes place during the β relaxation mode, while the randomization of the bond orientation is associated with the α modes. The intrinsic distribution captures the structural changes occurring during the β relaxation only. This is evident in the small variation of the intrinsic stresses during this regime. Neither the intrinsic stress nor the distribution changes during the α relaxation. This observation lays the foundation for the definition of the stress optical coefficient on structural grounds.

The Stress Optical Coefficient. The SOC or the ratio of birefringence to stress is defined in the intrinsic framework as the ratio of P_2 to the atom-based stress.[14] The global stress difference defined by $\sigma = t_{11} - (t_{22} + t_{33})/2 = (3/2)^{\mathrm{D}}t_{11}$is expressed in terms of the deviatoric intrinsic stresses ${}^{\mathrm{D}}\tilde{\sigma}_{ii} = \tilde{\sigma}_{ii} - (\tilde{\sigma}_{11} + \tilde{\sigma}_{22} + \tilde{\sigma}_{33})/3$ as[7,14]

$$\sigma = \sigma^{\mathrm{b}} + \sigma^{\mathrm{nb}} = CP_2(\theta_{\mathrm{b}}) \tag{9}$$

where

$$C = \frac{3}{2}[\rho_{\mathrm{b}}\,{}^{\mathrm{D}}\tilde{\sigma}_{11}^{\mathrm{b}} + \rho_{\mathrm{a}} D\,{}^{\mathrm{D}}\tilde{\sigma}_{11}^{\mathrm{nb}}] \tag{10}$$

The global atom-based stress in eq 9 is computed as the sum of contributions due to bonded and nonbonded interactions and is proportional to P_2 during the α mode. The proportionality constant C is the inverse of the SOC ($C = 1/\mathrm{SOC}$). The bond and atom number densities are represented by ρ_{b} and ρ_{a}, respectively, while ${}^{\mathrm{D}}\tilde{\sigma}_{11}^{\mathrm{b}}$ and ${}^{\mathrm{D}}\tilde{\sigma}_{11}^{\mathrm{nb}}$ represent the deviatoric intrinsic stresses due to bonded and nonbonded interactions. Hence, the SOC was shown to be constant during the α relaxation mode and to vary during the β mode, similar to the evolution of the intrinsic stress tensor during relaxation.

The origin of constant D in eq 10 is still uncertain.[7] However, it was shown that D is chain length independent. Since the intrinsic stress tensor computed from chain inner atoms is also independent of this parameter, it follows that the SOC does not depend on molecular weight. This conclusion is in agreement with experimental observations.

The investigation of the title topic therefore requires the elucidation of the entropic vs the energetic nature of the intrinsic stresses and of the variation of constant D with temperature and density. These issues are discussed below.

4. Results

The *D* Constant. The variation of D with temperature at constant density was studied by nonequilibrium MD simulations in both the 4-atom and 200-atom chain systems. The constant D was previously shown to be chain length independent if stresses were computed from chain inner atoms only.[7] The stress difference of

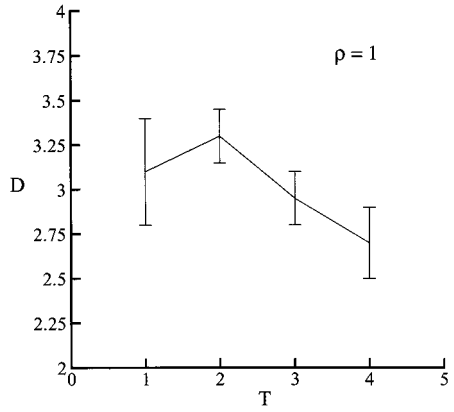

Figure 1. Variation of constant D with temperature for a system with density 1 (Lennard-Jones units).

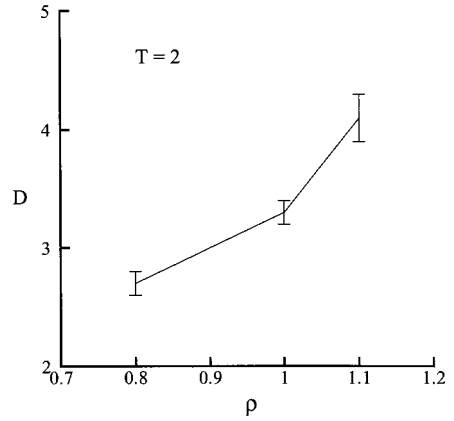

Figure 2. Variation of constant D with density at temperature $T = 2$ (Lennard-Jones units).

eq 9 as well as P_2 is computed in nonequilibrium simulations. The intrinsic stresses are evaluated in equilibrium simulations based on intrinsic distributions about chain inner atoms. Since the intrinsic stress tensor is independent of melt deformation during the α relaxation modes, there is no difference between results of equilibrium and nonequilibrium simulations. The constant D is then estimated from eq 10. An alternate method for the computation of D from equilibrium simulations is suggested in the following section.

Figure 1 shows the variation of D with temperature in a system of density 1 (Lennard-Jones units). The variation of D with density is shown in Figure 2 for a system at temperature $T = 2$. The error bars are estimated from the numerical and statistical uncertainties. The constant D appears to be weakly dependent on temperature within the accuracy of these simulations and for the investigated range of parameters. On the other hand, D varies significantly with density. The independence of D on temperature suggests that the entropic vs energetic character of the global stress at imposed P_2 (stretch) depends uniquely on the character of intrinsic stresses.

The Entropic Nature of Intrinsic Stress. Figure 3 shows the variation of the deviatoric intrinsic stress components due to bonded and nonbonded interactions, ${}^{D}\tilde{\sigma}_{11}^{b}$ and ${}^{D}\tilde{\sigma}_{11}^{nb}$ (eq 10), with temperature and for various system densities. The bonded deviatoric stress is strongly dependent on density and nonlinear with temperature. The nonbonded contribution, however, appears to be only weakly density dependent and linear with temperature. The individual components of the nonbonded intrinsic stress tensor $\tilde{\sigma}_{ii}^{nb}$ are strongly dependent on both density and temperature in a nonlinear fashion.[20] However, all components of the deviatoric tensor are density independent as shown in Figure 3 for ${}^{D}\tilde{\sigma}_{11}^{nb}$. Furthermore, it is possible to decompose ${}^{D}\tilde{\sigma}_{ii}^{nb}$ in two parts: one due to the nonbonded interactions of the representative atom with atoms belonging to other chains (interchain interactions) ${}^{D}\tilde{\sigma}_{ii}^{nb-ext}$ and the other due to interactions with atoms of the same chain (intrachain interactions) ${}^{D}\tilde{\sigma}_{ii}^{nb-int}$ or ${}^{D}\tilde{\sigma}_{ii}^{nb} = {}^{D}\tilde{\sigma}_{ii}^{nb-ext} + {}^{D}\tilde{\sigma}_{ii}^{nb-int}$. These components similarly exhibit a weak dependence on density and vary linearly with temperature.

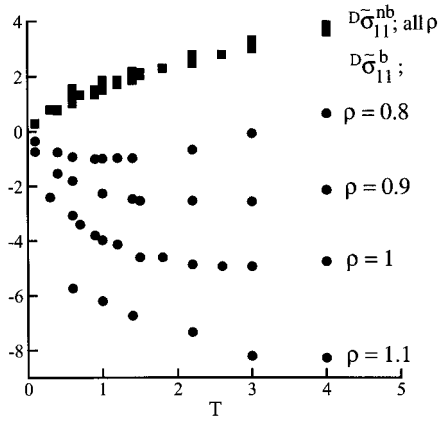

Figure 3. Variation of the deviatoric bonded and nonbonded intrinsic stress with temperature in systems with various densities. Intrinsic stresses are independent of chain length and are hence computed from the inner bond of 4-atom chains.

Figure 3 shows that neither the total deviatoric intrinsic stress ${}^{D}\tilde{\sigma}_{11}$ nor its two components, ${}^{D}\tilde{\sigma}_{11}^{b}$ and ${}^{D}\tilde{\sigma}_{11}^{nb}$, are purely entropic. The nonbonded deviatoric intrinsic stress is predominantly entropic with a small energetic component. However, the bonded deviatoric intrinsic stress is predominantly energetic at higher temperatures.

The Bonded Component. It is further useful to restrict attention to the nonbonded component of the deviatoric intrinsic stress. The bonded component can be expressed in terms of quantities related to nonbonded interactions. The bonded deviatoric intrinsic stress is given by the virial formula as

$$ {}^{D}\tilde{\sigma}_{11}^{b} = \frac{2}{3}\langle f^{b} b \rangle \tag{11} $$

where b is the current bond length and f^{b} is the force in the bond due to bonded interactions. With the force computed from eq 1, eq 11 becomes

$$ {}^{D}\tilde{\sigma}_{11}^{b} = \frac{2}{3}\left(b_0 \langle f^{b} \rangle + \frac{1}{\kappa}\langle (f^{b})^2 \rangle \right) \tag{12} $$

The average force $\langle f^{b} \rangle$ is related to the force $\langle f^{nb} \rangle$ in the direction of the bond due to nonbonded interactions by[21]

$$ \langle f^{b} \rangle + \langle f^{nb} \rangle = \frac{2k_B T}{b_0} \tag{13} $$

and hence, eq 12 can be written in terms of the

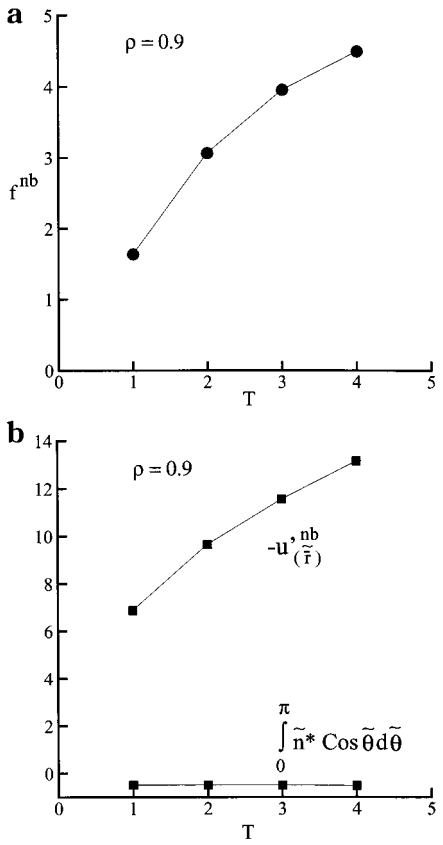

Figure 4. (a) Force in the bond direction due to nonbonded interactions as a function of temperature in the system with $\rho = 0.9$. (b) Components of the nonbonded force in (a) (Lennard-Jones units).

nonbonded force as

$$ {}^{\mathrm{D}}\tilde{\sigma}_{11}^{\mathrm{b}} = \frac{2}{3}\left[2k_{\mathrm{B}}T + \frac{4{k_{\mathrm{B}}}^2T^2}{\kappa {b_0}^2} - \left(b_0 + \frac{4k_{\mathrm{B}}T}{\kappa b_0}\right)\langle f^{\mathrm{nb}}\rangle_{(\rho,T)} + \frac{1}{\kappa}\langle (f^{\mathrm{nb}})^2\rangle_{(\rho,T)}\right] \quad (14) $$

Since the bonded and the nonbonded contributions are related by eq 13, it is sufficient to focus attention on one of them. Furthermore, eq 14, in conjunction with Figure 4a, justifies the parabolic variation of the bonded intrinsic deviatoric stress with temperature (Figure 3).

The variation of $\langle f^{\mathrm{nb}}\rangle$ with temperature is shown in Figure 4a for the system of density 0.9. The function is linear for $T < 3$ and tends to level off at higher temperatures. The structural origins of this behavior (and hence of the temperature dependence of ${}^{\mathrm{D}}\tilde{\sigma}_{11}^{\mathrm{b}}$) may be evidenced by writing f^{nb} in terms of the intrinsic distribution of nonbonded interacting neighbors,

$$ \langle f^{\mathrm{nb}}\rangle = -2\pi\int_0^{R_c}\int_0^{\pi} {u_{(\tilde{r})}}^{\mathrm{nb}\prime}\tilde{n}_{(\tilde{r},\tilde{\theta})}\tilde{r}^2 \sin\tilde{\theta}\cos\tilde{\theta}\,\mathrm{d}\tilde{\theta}\,\mathrm{d}\tilde{r} \quad (15) $$

where $\tilde{n}(\tilde{r},\tilde{\theta})$ is the nonbonded neighbors number density in intrinsic coordinates, while $\tilde{r}$ and $\tilde{\theta}$ are the radial and angular coordinates in the intrinsic frame. The function u^{nb} represents the nonbonded interaction potential. The intrinsic distribution here is that obtained after averaging over the population and all N_c replicas considered in the simulation.

Equation 15 can be simplified by collapsing the radial dimension of the distribution function and by projecting

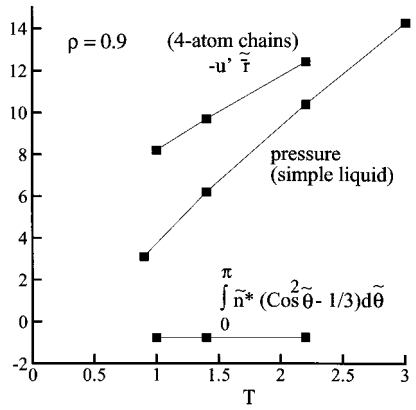

Figure 5. Components of the deviatoric nonbonded intrinsic stress as a function of temperature for the system with $\rho = 0.9$. The simple liquid pressure variation with temperature for $\rho = 0.9$ is also shown (Lennard-Jones units).

it on a sphere of radius $\tilde{r}$, where $\tilde{r}$ is the average distance between the representative atom and interacting nonbonded neighbors. Furthermore, it has been observed that $\tilde{r}$ is largely independent of $\tilde{\theta}$, which allows for separation of variables in eq 15:[8]

$$ \langle f^{\mathrm{nb}}\rangle \approx -{u_{(\tilde{r})}}^{\mathrm{nb}\prime}\int_0^{\pi}\tilde{n}^*(\tilde{\theta})\cos\tilde{\theta}\,\mathrm{d}\tilde{\theta} \quad (16) $$

The function $\tilde{n}^*(\tilde{\theta})$ is related to $\tilde{n}(\tilde{r},\tilde{\theta})$ and represents the number of neighbors in a conical sector centered on $\tilde{\theta}$ and of span $\mathrm{d}\tilde{\theta}$. The integral in eq 16 accounts for the steric shielding effect, while the $\tilde{\theta}$-independent factor in front of the integral accounts for packing. The variation of each of these terms with temperature is shown in Figure 4b (system density $\rho = 0.9$). The steric shielding effect is independent of temperature, while packing is highly sensitive to it. The packing effect therefore controls the temperature dependence of $\langle f^{\mathrm{nb}}\rangle$ and ${}^{\mathrm{D}}\tilde{\sigma}_{11}^{\mathrm{b}}$ with temperature.

The Nonbonded Component. The nature of the nonbonded deviatoric intrinsic stress is revealed by a similar approach. The stress ${}^{\mathrm{D}}\tilde{\sigma}_{11}^{\mathrm{nb}}$ is expressed in terms of the intrinsic distribution function, and further, the volume integral is approximated by factoring the $\tilde{r}$- and $\tilde{\theta}$-dependent terms. The nonbonded deviatoric stress is obtained as

$$ {}^{\mathrm{D}}\tilde{\sigma}_{11}^{\mathrm{nb}} \approx -{u_{(\tilde{r})}}^{\mathrm{nb}\prime}\tilde{r}\int_0^{\pi}\tilde{n}^*(\tilde{\theta})(\cos^2\tilde{\theta} - 1/3)\,\mathrm{d}\tilde{\theta} \quad (17) $$

Figure 5 shows the variation of the two components of eq 17 (that dependent on $\tilde{r}$ and that function of $\tilde{\theta}$ only) with temperature, for the system of density 0.9. Once again, the steric shielding effect is largely temperature insensitive, while the temperature variation of stress is due to packing effects. Furthermore, the packing-induced entropic character of ${}^{\mathrm{D}}\tilde{\sigma}_{11}^{\mathrm{nb}}$ is similar to that of pressure in simple liquids. The temperature variation of the pressure computed in the equivalent simple liquid (having the same density and the same potential cutoff radius) is shown in Figure 5. This curve is identical to the equation of state derived for Lennard-Jones liquids by Nicolas et al.[22] The entropic component (slope of the curve) of the simple liquid pressure is similar to that of the pressure computed in the polymeric system and due to nonbonded interactions only.

The Total Stress Difference σ. Attention is next focused on the global stress and the SOC. The predic-

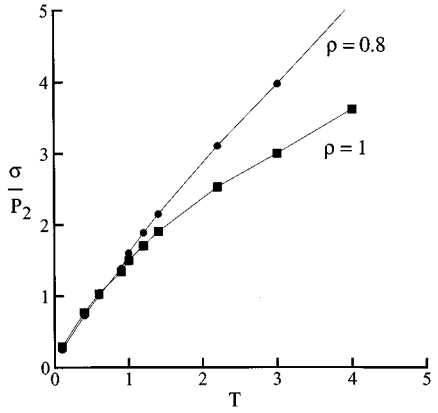

Figure 6. Variation of the ratio of the stress difference σ to P_2 (during α relaxation) with temperature for $\rho = 0.8$ and 1, based on predictions of eq 10 and with data in Figures 1 and 3.

tions of eq 10 based on the data presented in Figures 1 and 3 are plotted in Figure 6 for systems of density 0.8 and 1. The global stress at imposed P_2 appears to be purely entropic at temperatures below 1.3. Furthermore, the SOC defined by eq 10 varies linearly with temperature at low densities, similar to the predictions of the Rouse model. At higher density and temperature, the SOC becomes nonlinear. The nonlinear behavior of the SOC with temperature is in agreement with some experimental observations.[17]

Equation 9 for the global stress difference σ is valid only in the α relaxation regime, when the system is close to equilibrium. Stress in this regime is known to be entropic, and in this sense, the data in Figure 6 confirm that the intrinsic formulation is able to capture this behavior. Classically, based on the entropic spring model, stress in this regime is entropic by definition, and the entropic character is understood to be due to the conformation entropy of the chains. Here, the entropic character is an outcome rather than an assumption of the model and is rooted in the packing entropy in a manner similar to the simple liquid case. The picture holds for small- and large-molecular systems and for non-Gaussian chains, with the SOC being chain length independent.

The observation that the global stress difference σ is purely entropic (during the α relaxation mode) suggests a method for computing the constant D from equilibrium simulations. Accordingly, the intrinsic stresses are computed in equilibrium as functions of temperature and D is chosen such to render σ in the melt state (eq 9, eq 10, and Figure 3) purely entropic at low temperatures.

Finally, it is necessary to discuss the behavior of the system close to and below the glass transition temperature. Experimental data[17] show that the SOC undergoes a sharp variation at T_g and becomes a constant of temperature below this threshold. In the glassy state, stress is primarily energetic and molecular reorientation due to stress (stretch) is independent of temperature because thermally activated monomer rotations are unlikely. In the intrinsic framework, the intrinsic stresses vary significantly with deformation in the glassy state due to the change in shape of the "cage" of a representative atom (an energetic effect). The amount of "cage" shape change and the deformation-induced bond orientation is largely independent of temperature in this case. This property is, in turn, conveyed to the SOC.

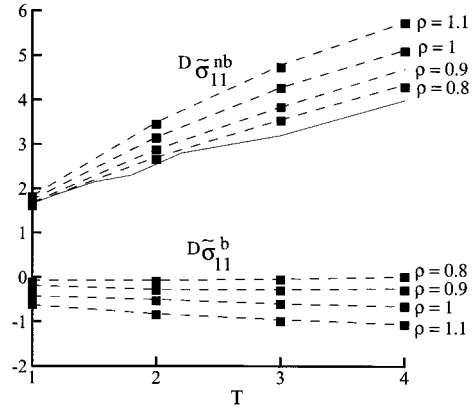

Figure 7. Variation of the bonded and nonbonded deviatoric intrinsic stress with temperature in systems with $\rho = 0.8$, 0.9, 1, and 1.1 and with stiffer bonded potential. Bond stiffness κ is 10 times larger than that of the system considered in Figure 3. The nonbonded deviatoric intrinsic stress from Figure 3 and for $\rho = 1$ is included for reference (continuous line).

Role of Model Parameters. The role of the model parameters in determining the conclusions discussed above needs to be analyzed. The sensitivity of the results to the bond stiffness κ, the bond length b_0, and the cutoff radius of the interatomic potential describing nonbonded interactions R_c are discussed below.

The Bond Stiffness κ. The effect of increasing the stiffness of the potential describing bonded interactions (eq 1) is shown in Figure 7 for systems of various densities. The nb curve ($\rho = 0.9$) from Figure 3 is reproduced for reference. The bonds in this model are in compression, as evidenced by the sign of the bonded stress in Figure 3. This is contrary to the prediction of the entropic spring model in which the chains are considered by default to be in tension. Stiffer bonds lead to neighboring bonded atoms being farther apart and therefore to weaker steric shielding. This, in turn, favors a more close-packed nonbonded distribution, with $\tilde{\bar{r}}$ decreasing. These two mechanisms have opposite effects on the magnitude of the intrinsic stresses. A detailed study of the intrinsic distribution reveals that $\tilde{n}^*(\tilde{\theta})$ is less affected by the variation of κ than is $\tilde{\bar{r}}$. Hence, the nonbonded deviatoric stress increases with increasing bond stiffness due to the closer packing (decrease in $\tilde{\bar{r}}$), while the magnitude of the bonded deviatoric stress decreases due to the limited deformation of the stiffer bonds.

Because of the enhanced role of packing, the energetic component of both bonded and nonbonded deviatoric intrinsic stresses decreases, while the entropic component of the nonbonded stress increases. The purely entropic character of the global stress difference σ is preserved.

The Bond Length b_0. The mechanism discussed above was verified by increasing the equilibrium bond length b_0. Figure 8 shows the bonded and the nonbonded deviatoric intrinsic stresses computed in a system with $\rho = 0.9$ and with bond length $b_0 = 1.1$. The corresponding data from Figure 3 are reproduced for reference. The increase in bond length leads to a behavior qualitatively similar to that discussed above for the case in which the bond stiffness is increased.

Larger Cutoff Radius R_c. Hard-sphere systems are known to be purely entropic. On the other hand, the pressure in soft-sphere systems such as simple liquids has a well-defined energetic component. It is therefore

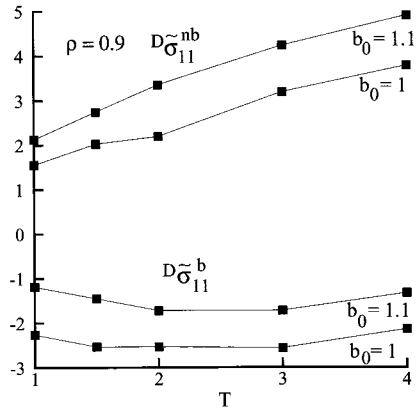

Figure 8. Variation of the nonbonded deviatoric intrinsic stresses with temperature in a system with $\rho = 0.9$ and with longer bonds ($b_0 = 1.1$). The data from Figure 3 for the system of same density and bond length $b_0 = 1$ are also shown.

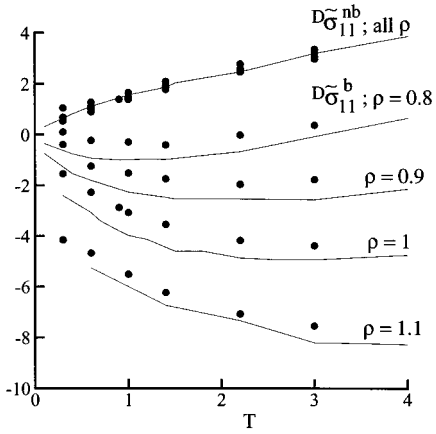

Figure 9. Variation of the deviatoric bonded and nonbonded intrinsic stress with temperature in systems with density $\rho =$ 0.8, 0.9, 1, and 1.1 and in which the nonbonded potential has both a repulsive and an attractive component (cutoff radius $R_c = 1.3$)—data points. The lines represent data from Figure 3 corresponding to the purely repulsive system.

expected that purely repulsive systems are largely entropic. Increasing the stiffness of the repulsive nonbonded potential in a soft-sphere system should lead to a more pronounced entropic character. Although this trend has been observed, it has been shown that the convergence is slow and the hard-sphere situation is not recovered, even for extremely repulsive potentials.[23] These observations suggest that the cutoff radius of the nonbonded potential may be a significant parameter in the present discussion.

Figure 9 shows the bonded and the nonbonded deviatoric intrinsic stresses (data points) computed in a system in which the nonbonded potential has an attractive component ($R_c = 1.3$). Data from Figure 3 (continuous lines) corresponding to the purely repulsive system are also shown. The nonbonded deviatoric stress is insensitive to the variation of R_c, while the bonded component is weakly sensitive to it. This is a consequence of the nonbonded deviatoric stress being primarily due to close range interactions and to steric shielding.[8] Since the constant D changes slightly with R_c, the total stress difference σ is again purely entropic in this system.

5. Conclusions

The present simulations performed on model polymeric melts have shown that the atom-based formulation captures the experimentally observed entropic nature of stress as well as several important features of the SOC. Stress in this framework is due to the excluded volume and is purely entropic. Its entropic nature is due to the packing effect. However, none of the individual components of the global stress difference are purely entropic. By contrast, in the classical model based on the entropic spring concept, the global stress is due to the chains being regarded as entropic springs in tension, while its entropic character is postulated (or imposed by the thermodynamics of the system). Furthermore, experiments show that the SOC is independent of the molecular weight, the deformation strain rate, and the presence of a solvent. The SOC computed from the atom-based stress within the intrinsic framework is also independent of the chain length and of melt deformation during the α relaxation modes. The effect of the solvent has not been investigated in this study. The SOC in the melt state is reported to be both dependent[16,17] and independent[12,15] of temperature in various material systems and is predicted to vary linearly with temperature by the entropic spring model. The SOC is observed to become nonlinear with temperature at high temperatures. In the present formulation, the SOC has a similar dependence on temperature. Finally, the intrinsic framework captures, qualitatively, the behavior of the SOC below the glass transition temperature.

Acknowledgment. This work was supported by the NSF through Grant CMS-9908025. The author thanks Professor J. H. Weiner for seminal discussions and encouragement.

References and Notes

(1) Rouse, P. E. *J. Chem. Phys.* **1953**, *21*, 1272−1285.
(2) Doi, M.; Edwards, S. F. *The Theory of Polymer Dynamics*; Clarendon: Oxford, 1986.
(3) Bird, R. B.; Curtis, C. F.; Armstrong, R. C.; Hassager, O. *Dynamics of Polymeric Liquids: Kinetic Theory*; Wiley-Interscience: New York, 1987.
(4) Gao, J.; Weiner, J. H. *Macromolecules* **1996**, *29*, 6048−6055.
(5) Gao, J.; Weiner, J. H. *Macromolecules* **1992**, *25*, 3462−3467.
(6) Loriot, G.; Weiner, J. H. *J. Polym. Sci., Polym. Phys.* **1998**, *36*, 143−154.
(7) Picu, R. C.; Loriot, G.; Weiner, J. H. *J. Chem. Phys.* **1999**, *110*, 4678−4686.
(8) Picu, R. C. *Macromolecules* **1999**, *32*, 7319−7324.
(9) Gao, J.; Weiner, J. H. *J. Chem. Phys.* **1989**, *90*, 6749−6760.
(10) Gao, J.; Weiner, J. H. *Science* **1994**, *266*, 748−751.
(11) Fixman, M. *J. Chem. Phys.* **1991**, *95*, 1410−1423.
(12) Kroger, M.; Luap, C.; Muller, R. *Macromolecules* **1997**, *30*, 526−539.
(13) Picu, R. C.; Weiner, J. H. *J. Chem. Phys.* **1998**, *108*, 4984−4991.
(14) Gao, J.; Weiner, J. H. *Macromolecules* **1994**, *27*, 1201−1209.
(15) Muller, R.; Pesce, J. J. *Polymer* **1994**, *35*, 734−739.
(16) Retting, W. *Colloid Polym. Sci.* **1979**, *257*, 689−698.
(17) Tobolsky, A. V. *Properties and Structure of Polymers*; Wiley: New York, 1960.
(18) Berendsen, H.; Postma, J.; van Gunsteren, W. *J. Chem. Phys.* **1984**, *81*, 3684−3693.
(19) Swenson, R. W. *Am. J. Phys.* **1987**, *55*, 746−751.
(20) Gao, J.; Weiner, J. H. *Macromolecules* **1991**, *24*, 1519−1525.
(21) Gao, J.; Weiner, J. H. *Mol. Phys.* **1990**, *70*, 299−318.
(22) Nicolas, J. J.; Gubbins, K. E.; Streett, W. B.; Tildesley, D. J. *Mol. Phys.* **1979**, *37*, 1429−1454.
(23) Heyes, D. M. *J. Phys. (Paris)* **1994**, *6*, 6409−6419.

MA002186S